STABLE CRACK GROWTH OF SURFACE CRACKS IN COMPONENTS

Wolfgang Brocks*

Some fundamental aspects of ductile, stable growth of cracks in components (pressure vessels and pipes) are discussed. Even for rather simple geometries like cylinders, the safety assessment of components still offers a number of problems depending on the loading configuration and the crack shape. Whereas only an averaged crack extension is determined in specimen tests, the local propagation of cracks may be of main importance for surface cracks in thick-walled pressure vessels and pipes. Some results of large scale tests and corresponding numerical analyses are presented.

INTRODUCTION

Cracks in components subjected to cyclic or static loading may grow subcritically (stable) for some time and then become critical (unstable) under service conditions. The safety assessment of a detected or postulated flaw, i.e. a conservative prediction whether or not it will become critical within a given service interval, base on concepts of linear elastic or elastic plastic fracture mechanics. Especially the concept of Leak-Before-Break (LBB) is widely accepted as a means of assessing the susceptibility of pressurized components to failure by unstable crack propagation (1). When a crack through continued growth reaches a size at which it penetratres the wall and becomes detectable by leakage of the pressurizing medium without leading to a global failure of the component, this local failure is supposed to be safe. High effort is therefore put on the experimental investigation of surface cracks in pressurized components and on the development of estimation schemes for the prediction of stable crack growth.

The following considerations restrict to some phenomena of crack growth in ductile materials which are usually described by J-resistance curves. Whereas the initiation value is mostly found to be independent of the specimen geometry, $J(\Delta a)$-curves may vary with the shape and size of the speci-

* Fraunhofer-Institut für Werkstoffmechanik, Freiburg, Germany

mens, phenomena which are known for many years (2) but still unsolved and intensively discussed as "constraint effects in fracture" (3). No general criteria exist for applying these R-curves to flaws in components (4,5). A LBB analysis requires reliable tearing resistance data up to 100% of the remaining ligament (leak), which is beyond any accepted condition on J-control (see Schmitt et al. in (1)). The analysis also needs an assumption how the crack shape will develop during growth. It is commonly assumed that an axial surface flaw remains geometrically similar. But evidences exist from many experiments (6,7,8) that its shape may develop quite differently and expand in longitudinal direction under the surface more than in wall thickness direction. The consequences for a LBB analysis are evident.

The present paper mainly reports on some results of experimental and numerical investigations at the Bundesanstalt für Materialforschung und -prüfung (BAM) (9,10) and at the Fraunhofer-Institut für Werkstoffmechanik (IWM) (11,12) which are part of a German research program on fracture mechanics failure concepts for the safety assessment of nuclear components.

TESTING OF COMPONENTS

Within the research program, large scale tests have been performed on pipes under four-point bending (Fig 1a,b) and on pressure vessels (Fig. 2a) containing artificial flaws of different kinds, semi-elliptical (se), through (th) and part through (pt) cracks, located axially (ax) or circumferentially (cf), and of various sizes. The flaws were mashined, saw cut or spark eroded and, in most cases, sharpened by fatigue cracking, afterwards. The structures were then subjected to static loading, bending and/or internal pressure. Table 1 gives an overview of the test program. Table 2 summarizes the tube tests under four point bending, Table 3 and 4 the vessel tests with axial through and surface cracks, respectively. The component tests were accompanied by standard tests on C(T) specimens to obtain R-curves of the materials and by tests on other specimen geometries, for instance tensile panels with through or part through cracks to investigate effects of geometry and load configuration. In the following, some significant results are selected to point out characteristics of ductile stable crack growth.

As large scale tests on tubes and pressure vessels are expensive and, hence, do not allow a multiple specimen technique various attempts have been tried to realize similar loading conditions with simpler specimen geometries. Garwood et al (13) tested cruciform biaxially loaded tensile panels, and Wobst (14) used tensile panels with side notches (Fig. 2b) to simulate the constraint conditions in a vessel.

ANALYSIS

Any fracture mechanics analysis requires the calculation of a parameter characterizing the load intensity, which is the J-integral in the present case of ductile behaviour. J was calculated by 3D non-linear finite element (FE) analyses. Two examples of FE meshes are shown in Figs. 3a,b.

For a plane specimens with a straight fatigue crack, only average J values are "measured", that means calculated from the measured load vs. displacement records, and special arrangements like side-grooving are made to ensure that any variation of J along the crack front remains small and the crack approximately straight. But this is unrealistic for natural cracks in components, where the variation of J along the crack front and the local crack extension become important. These variations may look very different depending on the crack shape, structure geometry and load configuration. J may have a maximum in or close to the centre of the crack (Figs 4a,b,c) or outside of the centre (Fig 4d). As J is determined by the stresses and the crack length its maximum will be found at the point of highest stress level if the depth for a part through crack or the length of a through crack is approximatly constant, i.e. the circumferential crack in the pipe under bending (Fig. 4a) and the straight through crack in the pressure vessel (Fig 4b), or at the deepest point of a crack if the remote stress is approximately constant, i.e. the semi-elliptical surface crack in the pressure vessel (Fig. 4c). If a surface crack is subjected to bending the effects of stress gradients and varying crack depth interfere and shift the maximum of J somewhere between crack centre and free surface. (Fig 4d). Some bending effects are also visible in Fig 4c for the deep surface flaw in the wall of a pressure vessel.

The FE analyses also gave the chance to investigate the total stress and strain state in the structure. For example, Figs 5a,b show plots of the local triaxiality of the stress state, $h=\sigma_h/\sigma_e$, which had appeared to be a significant quantity for the prediction of local crack growth (15,16). Though the variation of J along the crack front of a surface flaw is quite different in the pressure vessel (Fig. 4c) and in the pipe (Fig. 4d), the variation of h looks rather similar. It will be shown later that and why the local crack growth will follow the h-variation rather than the J-variation.

As non-linear analyses of large scale components are expensive, approximate solutions for J are of economic interest. A number of approaches for various problems exist and only a few examples can be given here, more detailed informations will be found in (10).

Newman and Raju (17) have tabulated magnification functions $H(\Phi)$ for calculating stress intensity factors, K, for semi-elliptical surface flaws for many geometries and loading configurations. For a thin-walled vessel we have $K_I(\Phi) = p\,(R_i/t+1)\,\sqrt{\pi a}\,f(\Phi)\,H_o(\Phi)/Q^2(a/c)$ and $H_o(\Phi)$ is shown in Fig. 6a for two flaw geometries both after Newman and Raju and from FE analyses. Differences are due to the non-ideal shape of the real flaw. K can be converted into elastic J by $J_e=K^2/E'$, and in addition, a plastic zone correction $J_{ssy}=J_e(a+r_y)$ may be applied by $r_y=(\beta/\pi)(K/\sigma_y)^2$, according to Irwin's concept, with β depending on the stress state, $(1-2\nu)^2 \le \beta \le 1$. β may be assessed by assuming that the plastic zone penetrates the vessel wall, $2r_y=t-a$, at the plastic collapse pressure, $p_y=(\sigma_y/M)(t/R_i)$, where M is Folias' shell correction factor. The result is plotted in Fig. 6b showing a reasonable agreement of this approximation, $\beta=0.29$, with the FE result, even at $p/p_y=.99$.

In fracture testing of specimens, J is calculated from the area, A, under the load vs. COD curve by the η-factor. The same procedure has been applied to the analyzed components. Fig. 7a shows that an approximately linear relation with η=1.8 exists between $A(\Phi,V)=\int\sigma_b(\Phi,V)dV$ and $J(\Phi,V)$ for the pipe of Fig. 1b under bending. Beyond the collapse pressure p_y, $J(\Phi)$ for the surface crack in the pressure vessel of Fig. 2a is split into an elastic and a plastic part, $J=J_{ssy}+J_p$. The plastic contribution is given by $J_p(\Phi)=\eta_p(\Phi)A_p(\Phi)$ with $A_p=\int\sigma_m(\Phi,V)dV_p-\sigma_m V_p/2$, and Fig.7b shows that η_p is about 2. in the average but varying along the crack front. At least approximate values of J can be obtained by these formulas if test results of load and COD are available but no FE analysis.

DUCTILE CRACK GROWTH

Two central questions arise if the ductile crack growth in components shall be assessed.

- What specimens have to be taken to determine resistance curves which are appropriate for the failure assessment of a structure?
- How does the crack shape develop, and which R-curves have to be used to predict local crack growth?

Figs. 8a,b contribute partial answers to these questions with respect to the axial through crack in the pressure vessel. The J_R-curve obtained from the vessel tests (Table 3) according to a multiple specimen technique lies between that of compact specimens and centre cracked panels. A standard J_R-curve will therefore overestimate the crack growth by a factor of 2.5 to 3. The originally straight crack becomes thumb nail shaped as for smooth specimens, and the location of Δa_{max} is close to J_{max} (Fig. 4b).

Ductile crack growth of surface cracks is much more sophisticated. The crack may develop a canoe shape, (Figs. 9a,b) which does not even correspond with the variation of J along the crack front (Fig. 4c). Using a unique "material" J_R-curve will therefore yield quantitatively and qualitatively wrong predictions of $\Delta a(\Phi)$, Fig. 10a. These predictions may not even be "conservative" as overestimating Δa in wall thickness direction can be unconservative in a LBB analysis. Thus, a realistic prediction has to be based on J_R-curves which account for the varying triaxiality of the stress state (15,16,19). Figs. 5a,b have shown that the highest triaxiality will not be found in the centre of the crack, where the in-plane constraint is low due to the small ligament in thickness direction, but more or less close to the surface of the structure, as the in-plane constraint in axial or width direction is much higher. $J(\Delta a)$ curves of specimens with extremely different triaxiality, i.e. bending and tension, are necessary, at least, to obtain triaxiality dependent resistance curves by interpolation, which are then applied to the prediction or simulation of ductile crack growth by a FE analysis. The two examples (19,20) in Figs. 10a,b show a satisfactory agreement between test results and analyses.

SUMMARY

Some significant results of experimental and numerical investigations of stable crack growth in components have been selected to point out characteristics of ductile stable crack growth. Transferring R-curves from specimens to components is not a straight-forward process, and one has to be aware of the difference that will in general exist between laboratory test and field conditions. Research programs help to further elucidate these special conditions and to work out clear regulations for the application of fracture mechanics concepts.

REFERENCES

(1) Coleman, C.E. (ed), "Leak-Before-Break in Water Reactor Piping and Vessels", Ontario, 1989, Int. J. Pres. Ves. & Piping 43 (1990).

(2) Garwood, S.J., ASTM STP 677, Philadelphia, 1979, pp. 511-532

(3) Symposium on "Constraint Effects in Fracture, Indianapolis, 1990, ASTM STP 1171, Philadelphia, 1992

(4) McCabe, D.E., Landes, J.D. and Ernst, H.A., Trans. 7th SMiRT Conf. 1983, Vol. G, paper G2/4.

(5) Blauel, J.G., On the assessment of surface cracks, Proc. 4th Japanese-German Joint Seminar on Structural Strength and NDE Problems in Nuclear Engineering, Kanazawa, 1988.

(6) Pugh, C.E., HSST program quaterly report for Jan. to March 1983, NUREG/CR-3334, Vol 1, ORNL/TM-8787/V1, NRC Fin. No. B80119

(7) Milne, I. and Knee, N., Fatigue Fract. Engng. Mater. Struct. 9 (1986), pp. 231-257

(8) Wobst, K. and Krafka, H.: 14th MPA-Seminar, Stuttgart, 1988, Vol 2, Paper 41

(9) Aurich, D., BAM-Report 137, Bundesanstalt für Materialforschung und -prüfung, Berlin, 1987.

(10) Aurich, D., BAM-Report 174, Bundesanstalt für Materialforschung und -prüfung, Berlin, 1990.

(11) Schmitt, W., IWM-Report W 6/88, Fraunhofer-Institut für Werkstoffmechanik, Freiburg, 1989.

(12) Schmitt, W. and Brocks, W., IWM-Report W 7/91, Fraunhofer-Institut für Werkstoffmechanik, Freiburg, 1991.

(13) Garwood, S.J., Davey, T.G. and Creswell, S.L., Int. J. Pres. Ves. & Piping 36 (1989), pp. 199-224.

(14) Wobst, K.: private communication, BAM Berlin, 1992.

(15) Kordisch, H., Sommer, E. and W. Schmitt, Nuclear Engineering and Design 112 (1989), pp. 27-35.

(16) Brocks, W. and Künecke, G., "Defect Assessment in Components - Fundamentals and Applications", ed. J.G. Blauel and K.H. Schwalbe, Mechanical Engineering Publications, London, 1991, pp. 189-201

(17) Newman, J.N. and Raju, I.S., ASTM STP 791, 1983, pp. 293-298.

(18) Talja, H., Kordisch, H. and Hodulak, L., "Defect Assessment in Components - Fundamentals and Applications", ed. J.G. Blauel and K.H. Schwalbe, Mechanical Engineering Publications, London, 1991, pp. 1025-1039.

(19) Klemm, W., Memhard, D. and Schmitt, W., "Fracture Mechnics Verification by large-scale testing", ed. K. Kussmaul, EGF/ESIS Publication 8, Mechanical Engineering Publications, London, 1991, pp. 139-150.

(20) Brocks, W., Künecke, G. and Wobst, K., Int. J. Pres. Ves. & Piping 40 (1989), pp. 77-90.

TABLE 1 - Component Test Program

component, geometry	pipe		vessel		
d_o [mm]	880	192	1580		
t [mm]	40	23	40		
L [mm]	4000	2300	3000 (cyl. part)		
flaw	120°, cf, pt	se, cf, pt	ax, th	se, ax, pt	
Loading	4 PB	4 PB + p	p		
material	StE 460	X20CrMoV121	StE 460	20MnMoNi55	StE 460
R_{eL}, $R_{po.2}$ [MPa]	480	365	480	465	480
R_m [MPa]	640	790	640	610	640
test series No.	P1	P2	V1	V2	V3
number of tests	1	4	10	4	1

TABLE 2 - Pipe Tests under 4 Point Bending with Circumferential Flaws

Test No.	crack length $2c_o$ [mm]	depth a_o [mm]	test load M_{max} [MNm]	p [MPa]	crack extension Δa_{max} [mm]	collapse load M_{pl} [MNm]
P1	890	24	8.82	-	2.1	10.8
P2-1	24.2	12.3	0.88	10	1.0	
P2-2	40.2	16.0	0.83	10	2.7	0.35
P2-3	52.0	13.0	0.85	10	3.1	
P2-4	24.4	11.9	0.98	10	6.7	

TABLE 3 - Vessel Tests with Axial through Cracks

Test No.	crack length $2a_o$ [mm]	test pressure p_{max} [MPa]	crack extension Δa_{max} [mm]		collapse pressure p_F [MPa]
V1-1	104	18.6	0.35	-	23.8
V1-2	147	18.6	0.48	1.42	22.7
V1-4	251	15.6	0.25	0.90	19.6
V1-5	350	7.9	0.02	0.02	16.8
V1-6	450	8.4	-	0.68	14.4
V1-7	264	15.8	1.69	1.34	19.2
V1-8	303	14.7	1.90	2.00	18.1
V1-9	400	8.0	0.02	0.07	15.5
V1-10	463	8.8	0.83	0.76	14.1

TABLE 4 - Vessel Tests with Axial outer Surface Cracks

Test No.	crack length $2c_o$ [mm]	depth a_o [mm]	test pressure p_i [MPa]	p_{max} [MPa]	crack extension Δa_{max} [mm]	collapse pressure p_y [MPa]
V2-1	180.4	21.6	22.4	24.2	0.9	21.2
V2-2	184.8	26.8	20.1	25.5	0.6	19.2
V2-3	191.0	30.7	20.7	23.7	1.9	16.6
V2-4	203.7	35.9	19.4	24.5	3.2	10.2
V3-1	192.0	28.0	20.0	22.4	2.5	19.2

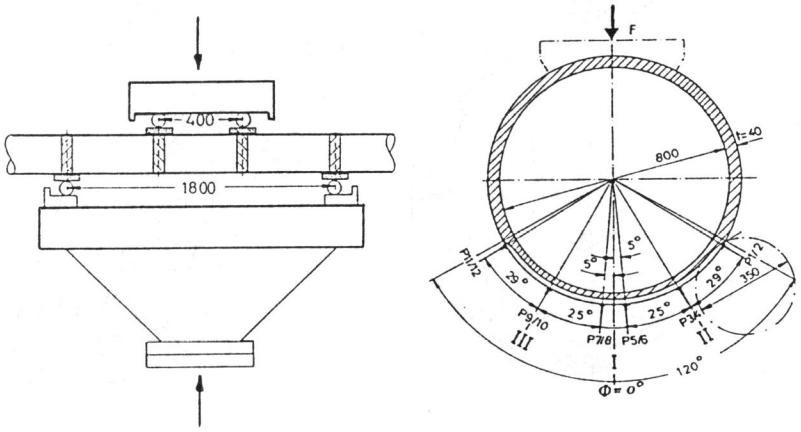

Figure 1 Pipe testing under four point bending
a) test device (11) b) pipe cross section for test P1 (10)

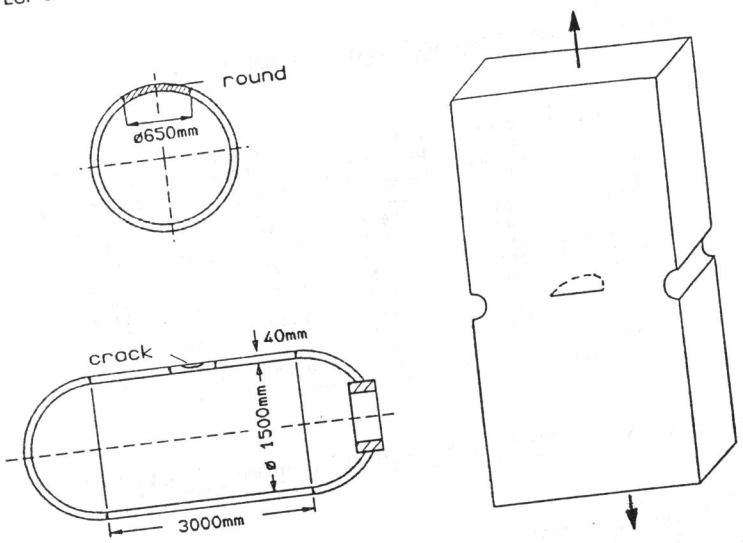

Figure 2 Structures with semi-elliptical surface flaws
a) pressure vessel (9,10) b) tensile panel with notches (14)

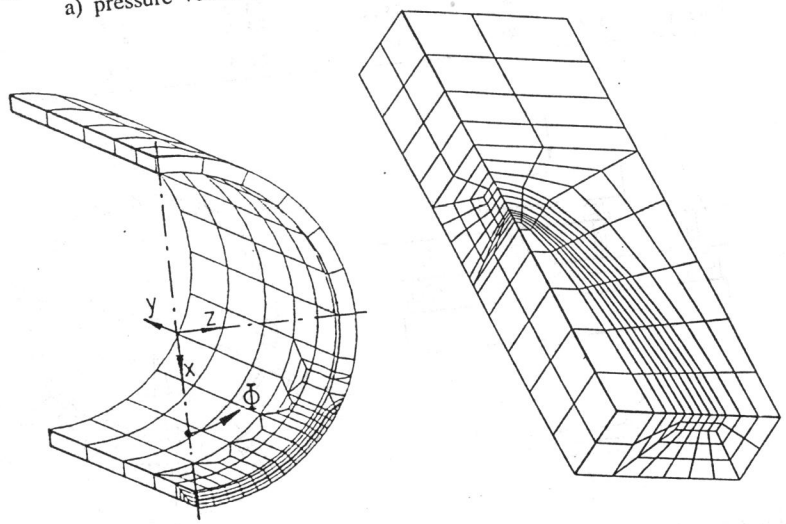

Figure 3 Finite element meshes
a) analysis of pipe test P1 (10) b) semi-elliptical flaw (12)

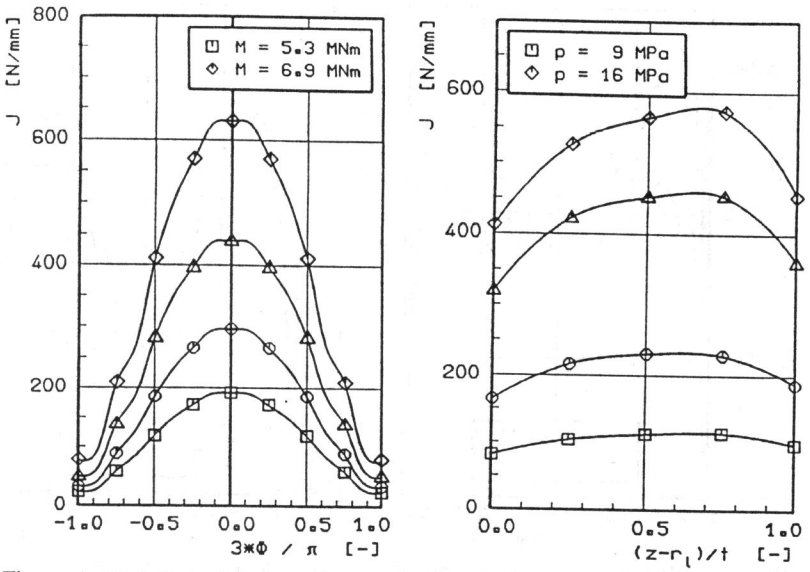

Figure 4 Variation of J along the crack front from FE-analyses
a) pipe test P1 (10) b) vessel test V1-4 (10)

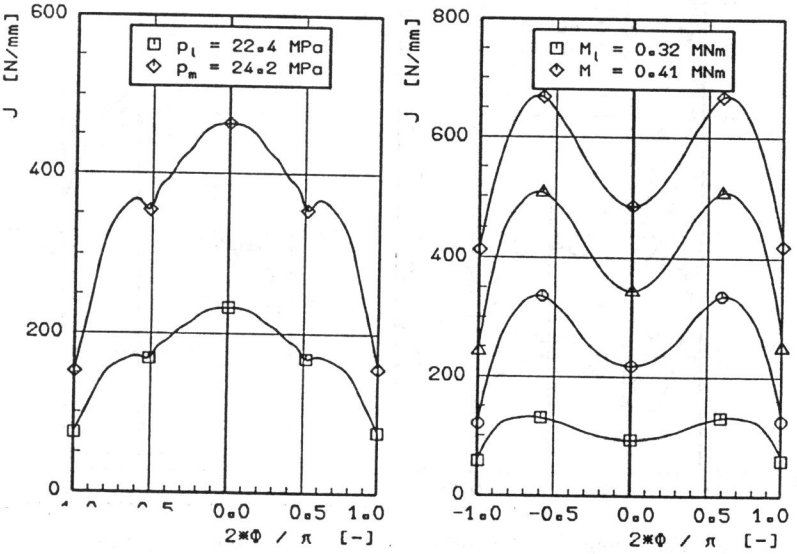

c) vessel test V2-1 (10) d) pipe test P2-4 (11)

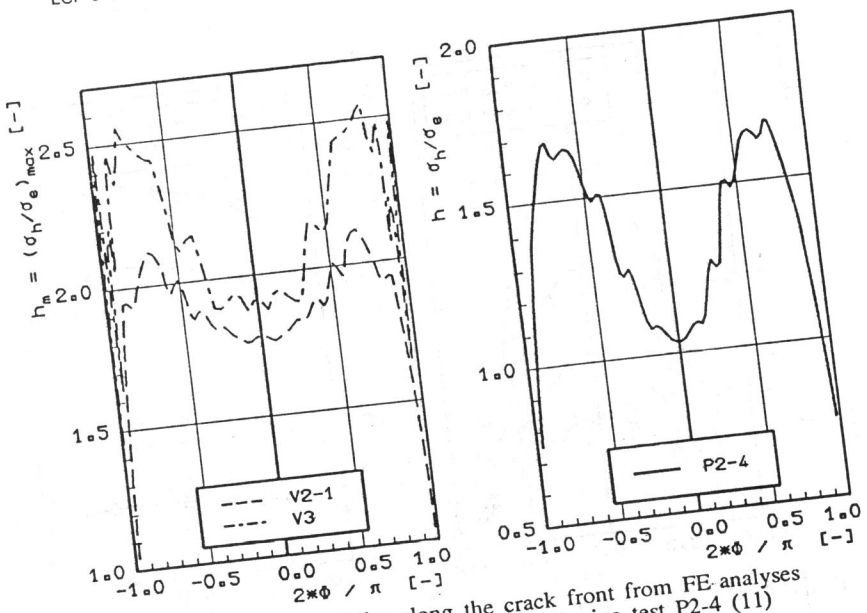

Figure 5 Variation of triaxiality along the crack front from FE analyses
a) vessel tests V2-1 and V3 (10) b) pipe test P2-4 (11)

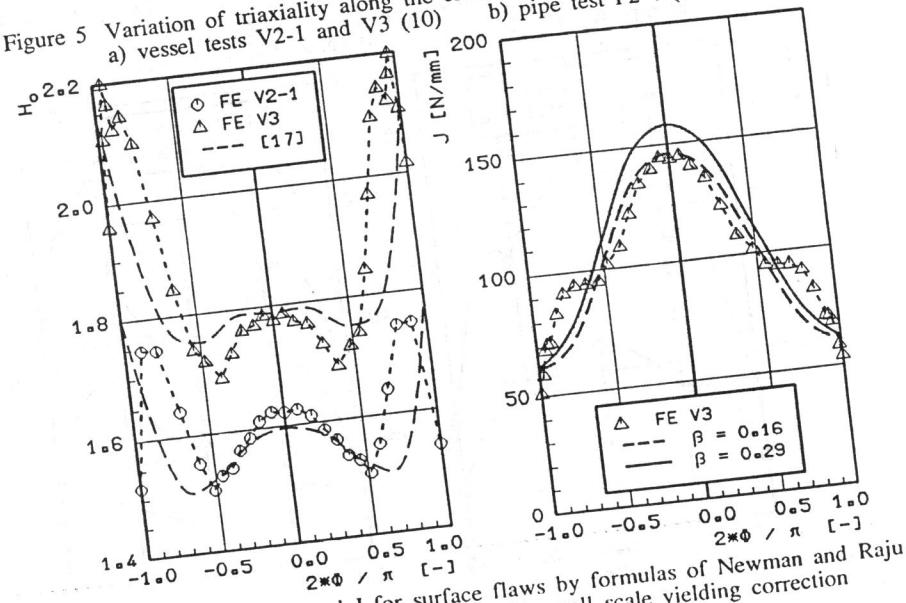

Figure 6 Estimating K and J for surface flaws by formulas of Newman and Raju
a) magnification function for K_I b) small scale yielding correction

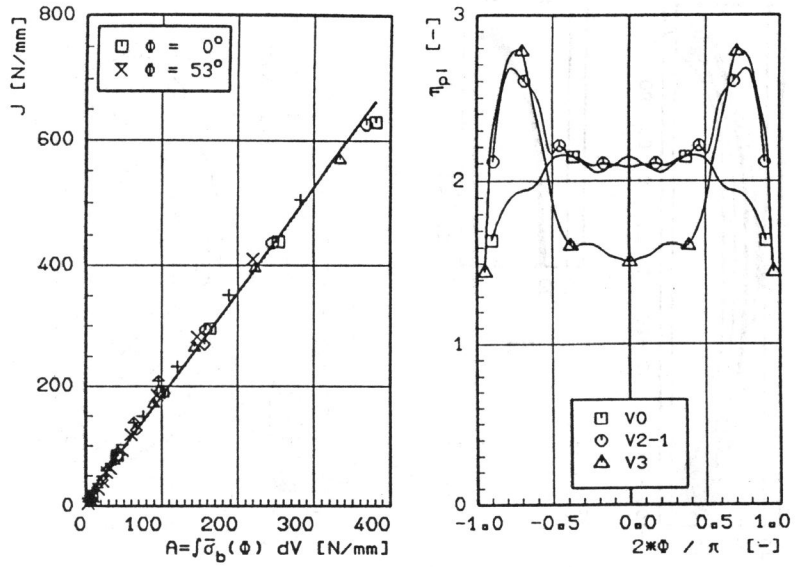

Figure 7 Application of η-method for calculating J
a) analysis of pipe test P1 b) analyses of various vessels

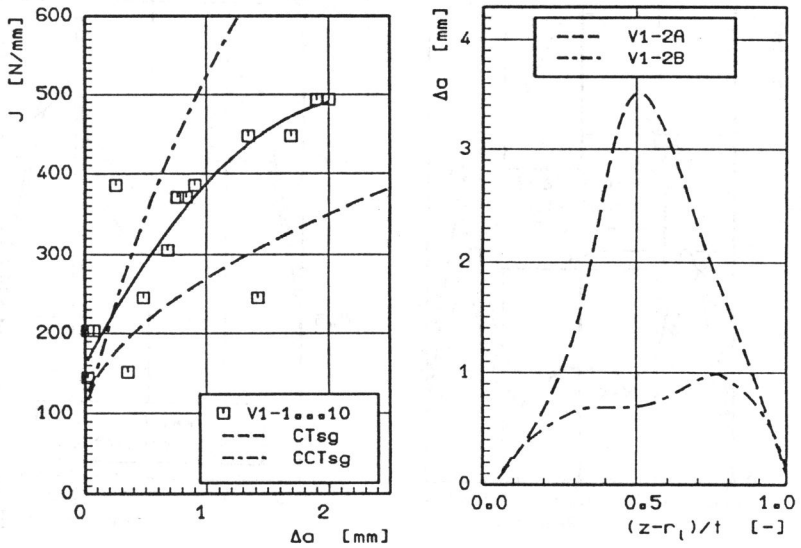

Figure 8 Vessel tests V1 with axial through cracks
a) J_R curves of vessel and specimens b) crack shape for V1-2

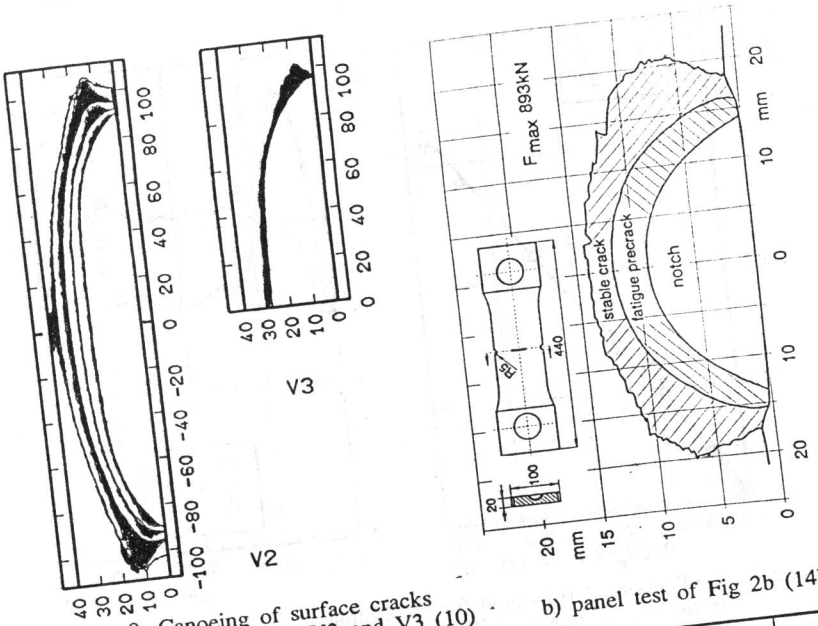

Figure 9 Canoeing of surface cracks
a) vessel tests V2 and V3 (10) b) panel test of Fig 2b (14)

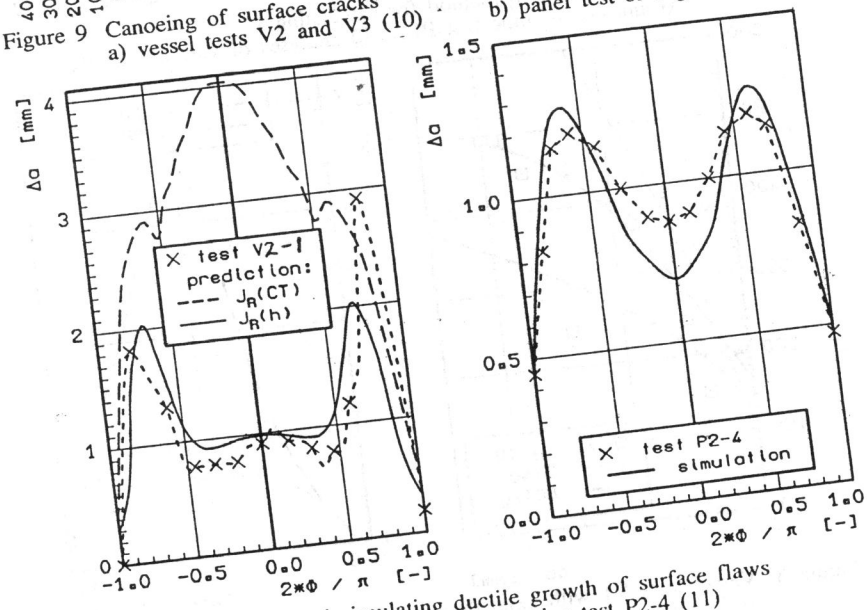

Figure 10 Predicting and simulating ductile growth of surface flaws
a) vessel test V2-1 (10) b) pipe test P2-4 (11)